



Title:

**A Hybrid Method of Geometric and Learning Techniques for Efficient Detection of ASFs from Sketches to Automatically Convert to 3D Models**

Authors:

Masaji Tanaka, [masaji-tanaka@ous.ac.jp](mailto:masaji-tanaka@ous.ac.jp), Okayama University of Science  
 Yueyang Zhao, [2115264808@qq.com](mailto:2115264808@qq.com), Okayama University of Science  
 Yangkun Wang, [r24smn6wp@ous.jp](mailto:r24smn6wp@ous.jp), Okayama University of Science  
 Enze Li, [lienze480@gmail.com](mailto:lienze480@gmail.com), Okayama University of Science  
 Rikuu Zenkai, [rikuu.zenkai@mebius-pkg.co.jp](mailto:rikuu.zenkai@mebius-pkg.co.jp), AKTIO Corporation  
 Masaaki Ohtsuki, [ohtsuki@aikoku.com](mailto:ohtsuki@aikoku.com), Aikoku Alpha Corporation  
 Chiharu Higashino, [higashino@aikoku.com](mailto:higashino@aikoku.com), Aikoku Alpha Corporation

Keywords:

Sketch, 3D model, Automatic Conversion, SFBCM, Sketch Feature, Abstract Sketch feature, machine learning, YOLO

DOI: 10.14733/cadconfP.2025.240-244

Introduction:

Sketches in the form of line drawings are commonly observed in magazines, books, and manuals, among others. Sketches are also important for designers, particularly mechanical designers, when inventing new ideas for products and their parts. The automatic conversion of sketches into 3D models will be advantageous for a variety of applications in CAD, CG, and computer vision. Over the last 50 years, numerous methods have been developed for the conversion, e.g. [2]. However, no conversion system has been developed to date. We have been developing methods for the conversion, and proposed a method called *Sketch Feature-Based Conversion Method* (SFBCM) to achieve the automatic conversion, limited to the sketches of mechanical objects, e.g. [10-12]. In SFBCM, each sketch is correctly drawn using 2D CAD systems and is an orthogonal projection of an opaque object viewed from a general perspective. Fig. 1 shows three basic *Sketch Features* (SFs) indicating a cuboid, cylinder, and round hole. Each can be recognized as a 3D object, and also drawn easily by humans. In SFBCM, when a sketch is input, its 3D model can be obtained by detecting and extracting SFs as 3D features step-by-step, and combining them in accordance with the sketch.

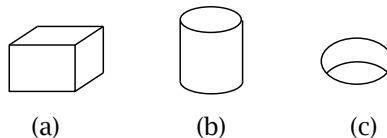


Fig. 1: Three basic SFs: (a) Cuboid, (b) Cylinder, and (c) Round hole.

An overview of SFBCM is explained using Example 1 shown in Fig. 2(a). When it is input to SFBCM, first, an SF of a cylinder ( $SF_1$ ) can be detected, and its hidden lines can be drawn as shown in Fig. 2(b). When  $SF_1$  is extracted as a 3D feature as shown in Fig. 2(c), two pink lines become isolated lines, each of which cannot form a closed loop of lines. In SFBCM, they are restored by their extension as shown in Fig. 2(d). In this figure, no SFs indicated in Fig. 1 can be detected. In this case, *Additional Lines* (ALs) are drawn to help detect SFs in SFBCM. To draw that, first, all junctions of line segments are recognized as shown in the figure. These are classified to  $L$ ,  $W$ ,  $T$ , and  $Y$ -junctions using the junction

dictionary, e.g. [3-4],[6]. Here, this naming was derived from the shapes of the alphabet, i.e., “L,” “W,” “T,” and “Y,” respectively. In the figure, there are five *L*-junctions, six *W*-junctions, three *T*-junctions, and three *Y*-junctions. ALs are drawn from *L*-, *W*-junctions. Each of two lines forming an *L*-junction is extended to the nearest solid line. Also, each of two lines in both sides of a *W*-junction is extended to the nearest solid line. The extended parts of the lines become ALs. Each extension continues until it intersects another line in a sketch; otherwise, it is removed. Consequently, five ALs (red lines) can be drawn from three *W*-junctions as shown in Fig. 2(e). In this figure, two SFs of a cuboid ( $SF_2$ ,  $SF_2'$ ) can be detected as shown in Fig. 2(f). Although both can be detected first, for a simpler explanation of this example,  $SF_2$  is detected and extracted as shown in Fig. 2(g). The search of the optimal sequence for detecting SFs has been being an issue in SFBCM. In this figure,  $SF_3$  is detected. After it is extracted, three isolated lines exist as shown in Fig. 2(h). However, their extension cannot form any SFs. In this case, the detection of *Abstract Sketch Features* (ASFs) is performed in SFBCM [11]. Each ASF expresses a part of an SF, and is made by cutting the SF. When an ASF is detected from a sketch, its corresponding SF can be predicted in SFBCM. Fig. 3 shows three ASFs made from SFs of a cuboid and cylinder. The isolated points of isolated lines are emphasized and colored red. Consequently, an ASF of a cuboid can be detected in Fig. 2(h). Fig. 2(i) shows the relationship between inferring SF from the ASF and  $SF_3$ . In SFBCM, the SF is predicted as  $SF_4$  as shown in Fig. 2(j) to contact the center of  $SF_3$ . Detailed prediction methods are described in [11]. When the 3D features of  $SF_1$ ,  $SF_2$ ,  $SF_3$ , and  $SF_4$  are combined in accordance with Fig. 2(a), the solution of Example 1 can be obtained as shown in Fig. 2(k). Although Example 1 can be solved by applying three SFs and an ASF, most of the sketches are more complex than it. Therefore, more SFs and their ASFs are required for the practical conversion system. In SFBCM, about a dozen SFs and their ASFs were defined. Fig. 4 shows a part of them. For example, the polygonal extrusion shown in Fig. 4(a) is defined as a polygon and several parallelograms; each line segment of the polygon can become a line segment of a parallelogram, and two adjacent parallelograms share a line segment. The definitions of the other SFs are found in [9]. However, it becomes difficult to detect an SF or ASF from a given sketch when their numbers are increased. For example, the SF of a cuboid can be defined as the three lines of three parallelograms that form a *Y*-junction. Therefore, it is not difficult to detect the SF in a sketch. However, it is difficult to detect an ASF like Fig. 3(a) because its definition will be more complex than the SF. Consequently, we attempt to apply existing machine learning techniques for the detection. In this paper, we propose a hybrid method of geometric and learning techniques for efficient detection of ASFs.

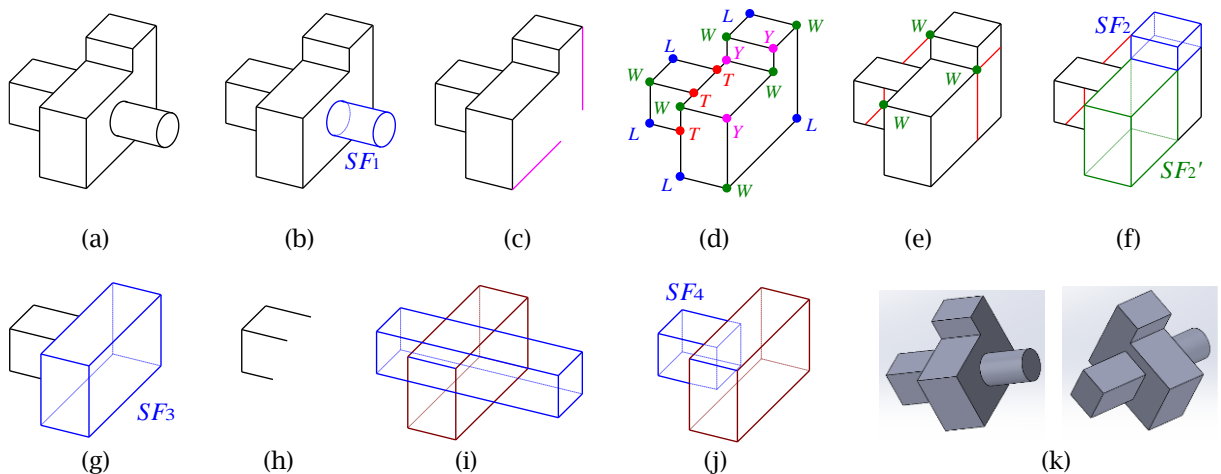


Fig. 2: (a) Example 1, (b) Detection of  $SF_1$ , (c) Extraction of  $SF_1$ , (d) Restoration of two isolated lines and recognition of all junctions of line segments, (e) Five ALs, (f) Detection of  $SF_2$  and  $SF_2'$  (g) Detection of  $SF_3$ , (h) Extraction of  $SF_3$  and detection of an ASF (i) Prediction of the ASF into an SF of a cuboid, (j) Detection of  $SF_4$ , and (k) Two overviews of the solution.

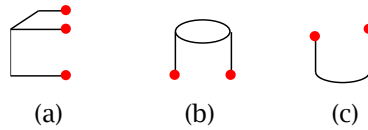


Fig. 3: Three ASFs: (a) ASF of a cuboid, (b) ASF of a cylinder, and (c) Another type of ASF of a cylinder.

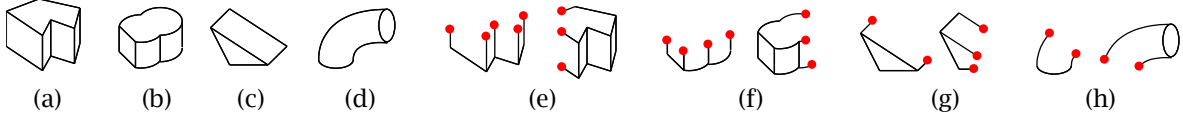


Fig. 4: Four SFs and their ASFs: (a) Polygonal extrusion, (b) Multiple extrusion, (c) Rib, (d) Pipe, (e) Two ASF types of (a), (f) Two ASF types of (b), (g) Two ASF types of (c), and (h) Two ASF types of (d).

### Main Idea:

Previously, we had proposed a method to automatically restore broken SFs using our inductive learning technique [8]. For example, the process to restore broken SFs of a cylinder can be learned and generalized. Although the method can give an accurate answer geometrically and theoretically, how to train a lot of restoration processes, how to apply it to resemble patterns, and how to implement the overall learning system has been ignored. In recent years, object detection systems based on convolutional neural networks have been actively developed, such as You Only Look Once (YOLO), e.g., [7]. We consider that detecting ASFs from CAD data, such as Drawing Exchange Format (DXF) data, is difficult, but from CAD image data using YOLO is not difficult, but efficient for SFBCM. In the present step of our study, the ASF of a cuboid and a cylinder has been trained using YOLOv11. The number of training data is 123 for the ASF of a cuboid and 128 for the ASF of a cylinder. The updated SFBCM with YOLO is explained using Example 2 shown in Fig. 5(a). When this figure is input to this method, an SF of a cylinder and two SFs of a cuboid are detected as shown in Fig. 5(b). In Fig. 5(c), these are extracted. In Fig. 5(d), an SF of a cuboid can be detected, and it is extracted in Fig. 5(e). In this figure, when all isolated lines are extended as shown in Fig. 5(f), no SFs can be detected. Therefore, in this case, ASF(s) is searched with YOLO. For its detection, all isolated points are emphasized as red points as shown in Fig. 5(g). When this figure is input as an image into YOLOv11, the output can be obtained as shown in Fig. 5(h). In this figure, it is found that an ASF of a cylinder (71% probability) and two ASFs of a cuboid (93%, 96% probability) are detected. The numerical data of the positions in the ASFs in the input image can be obtained from YOLO. Therefore, it can adjust to the positions of DXF data in this figure. Consequently, these three ASFs can be detected as DXF data correctly. Fig. 5(i) shows the prediction of them where each of two SFs are contacted centrally. Finally, the solution of Example 2 can be obtained by combining 3D features of five SFs of a cuboid and two SFs of a cylinder as shown in Fig. 5(j).

### Examples:

In this section, the effectiveness of this method is demonstrated using two examples. Fig. 6(a) shows Example 3 expressing a table. First, this method detects an SF of a cuboid as shown in Fig. 6(b). When the SF is extracted, no SFs can be detected. Therefore, isolated lines and points are detected as shown in Fig. 6(c). Although it is complex and difficult to detect each ASF from the DXF data of this figure, YOLOv11 is able to detect four ASFs of a cuboid from the image of the figure as shown in Fig. 6(d). Although the correct prediction of these ASFs into SFs is difficult in the present step of our study, if some learning system such as YOLO can easily infer that Example 3 represents a table automatically, its solution would be obtained.

Fig. 7(a) shows Example 4 expressing an *H*-section steel. Although it is possible to detect an SF of a polygonal extrusion from this figure, this detection will become difficult. Also, when ALs are drawn as shown in Fig. 7(b), two SFs of a cuboid can be simply detected. Therefore, when this example is input, first, an SF of a cuboid is detected as shown in Fig. 7(c) in this method. Fig. 7(d) shows the extraction of the SF. In this figure, three isolated lines are detected. It can be an ASF of a polygonal extrusion, but we do not have trained the ASF yet. So, ALs are drawn as shown in Fig. 7(e). When the image of this figure is input to YOLOv11, an ASF of a cuboid (97% probability) can be detected as shown in Fig. 7(f).

After the ASF is predicted into an SF of a cuboid, and it is extracted, another SF of a cuboid can be detected. Consequently, the solution can be obtained as shown in Fig. 7(g).

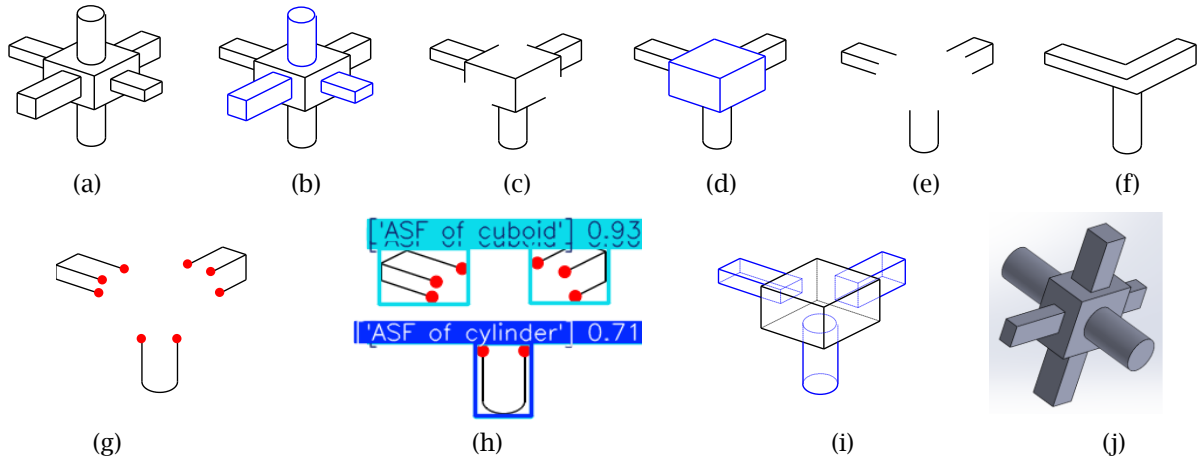


Fig. 5: (a) Example 2, (b) Detection of three SFs, (c) Extraction of them, (d) Detection of an SF of a cuboid, (e) Extraction of the SF, (f) Extension of all isolated lines, (g) Emphasis of isolated points, (h) Detection of three ASFs with YOLOv11, (i) Prediction of the ASFs into SFs, and (j) An overview of the solution.

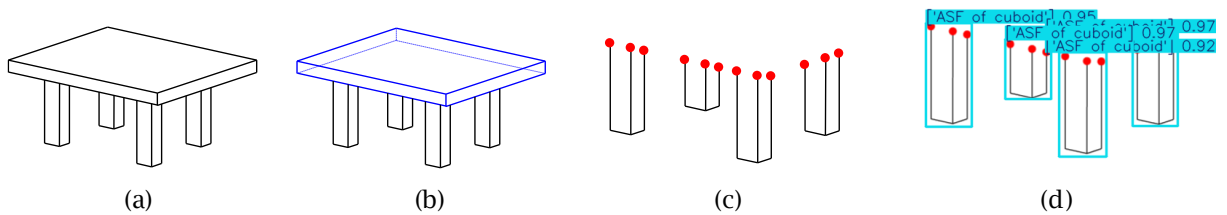


Fig. 6: (a) Example 3, (b) Detection of an SF of a cuboid, (c) Detection of isolated lines and points, and (d) Detection of four ASFs using YOLOv11.

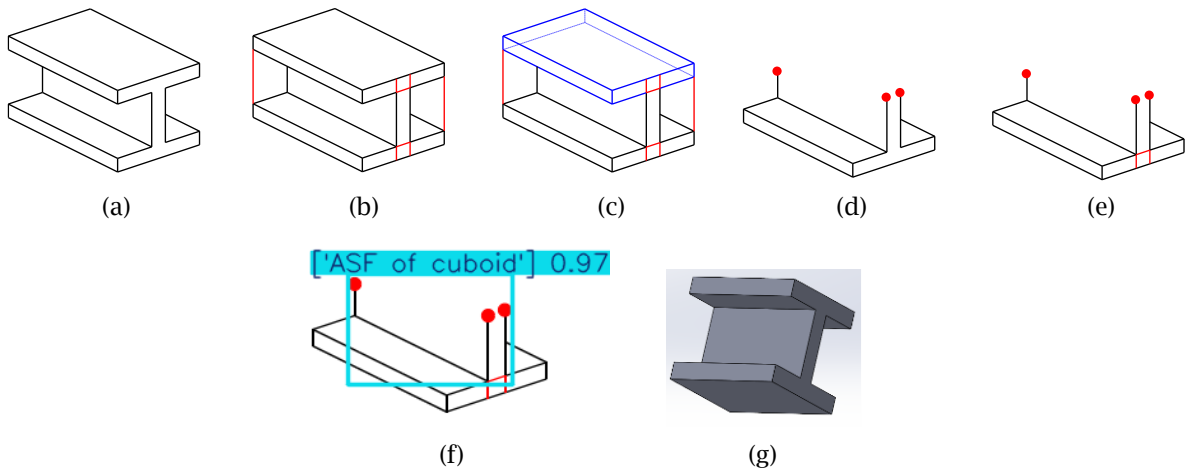


Fig. 7: (a) Example 4, (b) Drawn ALs, (c) Detection of an SF of a cuboid, (d) Extraction of the SF, (e) Drawn ALs, (f) Detection of an ASF of a cuboid, and (g) An overview of the solution.

### Conclusions:

In this paper, we propose a hybrid method of geometric and learning techniques for efficient detection of ASFs from sketches to automatically convert to 3D models. For the training of ASFs, we apply YOLOv11. The effectiveness of this method can be shown in three examples. For the efficient detection of SFs, we had already consider to draw *Second Additional Lines* (SALs) form ALs [13]. However, it is difficult to form an algorithm to how to draw them. Although it is found that this method is more effective than using SALs, their necessity would be remained in many cases of complex sketches. Consequently, more efficient formation and detection of SFs and ASFs, and more effective their training will become our challenges for realizing a practical conversion system. In recent years, the applications of machine learning techniques for the conversion are actively increasing, e.g. [1],[5]. However, they are not yet suitable for converting images of new creative objects into accurate 3D models. We believe that our hybrid technique is a current optimization technique that compensates for the shortcomings of individual techniques such as in CAD and CG.

Masaji Tanaka, <https://orcid.org/0000-0002-5266-9182>

### References:

- [1] Alhamazani, F.; Lai, Yu-Kun; Robin, Paul L.: 3DCascade-GAN: Shape completion from single-view depth images, *Computers & Graphics*, 115, 2023, 412-422. <https://doi.org/10.1016/j.cag.2023.07.033>
- [2] Camba, J. D.; Company, P.; Naya, F.: Sketch-Based Modeling in Mechanical Engineering Design: Current Status and Opportunities, *Computer-Aided Design*, 150, September 2022, 103283. <https://doi.org/10.1016/j.cad.2022.103283>
- [3] Clowes, M.B.: On seeing things, *Artificial Intelligence*, 2(1), 1971, 79-116. [https://doi.org/10.1016/0004-3702\(71\)90005-1](https://doi.org/10.1016/0004-3702(71)90005-1)
- [4] Huffman, D. A.: Impossible objects as nonsense sentences, *Machine Intelligence* 6, 1971, 295-323.
- [5] Liu, M; Shi, R.; Chen, L.; Zhang, Z.; Wei, X.: Fast Single Image to 3D Objects with Consistent Multi-View Generation and 3D Diffusion, 2024 IEEE/CVF Conference on Computer Vision and Pattern Recognition (CVPR). <https://doi.org/10.1109/CVPR52733.2024.00960>
- [6] Malik, J.: Interpreting line drawings of curved objects, *International Journal of Computer Vision*, 1, 1987, 73-103. <http://dx.doi.org/10.1007/BF00128527>
- [7] Redmon, J.; Divvala, S.; Girshick, R.; Farhadi, A.: You Only Look Once: Unified, Real-Time Object Detection, 2016 IEEE Conference on CVPR, 779-788. <https://doi.org/10.48550/arXiv.1506.02640>
- [8] Tanaka, M.; Terano, M.; Higashino, C.; Asano, T.; Takasugi, K.: A Learning Method for Reconstructing 3D Models from Sketches, *Computer-Aided Design & Applications*, 16(6), 2019, 1158-1170. <https://doi.org/10.14733/cadaps.2019.1158-1170>
- [9] Tanaka, M.; Terano, M.; Asano, T.; Higashino, C.: Method to Automatically Convert Sketches of Mechanical Objects into 3D Models, *Computer-Aided Design & Applications*, 17(6), 2020, 1168-1176. <https://doi.org/10.14733/cadaps.2020.1168-1176>
- [10] Tanaka, M.; Asano, T.; Higashino, C.: Isometric Conversion of Mechanical Sketches into 3D Models, 18(4), 2021, 772-785, <https://doi.org/10.14733/cadaps.2021.772-785>
- [11] Tanaka, M.; Asano, T.; Higashino, C.: Abstraction of Sketch Features for Predicting Hidden Shapes of Sketches for The Automatic Conversion into 3D Models, *Computer-Aided Design & Applications*, 19(5), 2022, 977-987. <https://doi.org/10.14733/cadaps.2022.977-987>
- [12] Tanaka, M.; Zenkai, R.; Liu, W.; Higashino, C.; Ohtsuki, M.: Convertible Sketches of Mechanical Curved Objects into 3D Models, *Computer-Aided Design & Applications*, 22(3), 2025, 400-413. <https://doi.org/10.14733/cadaps.2025.400-413>
- [13] Tanaka, M.; Zenkai, R.; Ohtsuki, M.; Higashino, C.: Effective Extraction of Sketch Features from Sketches for Converting to 3D Models in SFCBM, *Proceedings of CAD'24*, 2024, 376-380. <https://doi.org/10.14733/cadconfP.2024.376-380>